The Journal of Engineering

The 7th International Conference on Renewable Power Generation (RPG 2018)

IET Journals
The Institution of Engineering and Technology

SVD filtering and TLS-ESPRIT algorithm based on stator fault characteristic detection of doubly-fed induction generator

eISSN 2051-3305
Received on 26th October 2018
Accepted on 10th January 2019
E-First on 1st July 2019
doi: 10.1049/joe.2018.9265
www.ietdl.org

Boqiang Xu[1], Zehui Zheng[1] ✉

[1]*School of Electrical and Electronic Engineering, North China Electric Power University, Baoding 071003, Hebei, People's Republic of China*

✉ *E-mail: 1220031322@qq.com*

Abstract: This study proposes a novel method for detecting faults in the stator of the doubly-fed wind turbines based on the combination of singular value decomposition (SVD) filtering and least-squares parameter invariant signal technique (TLS-ESPRIT). The stator current signal and rotor current signal are simulated in the form of stator inter-turn short-circuit fault, and TLS-ESPRIT performance test is carried out. The results show that TLS-ESPRIT still has a high-frequency resolution for a short-time signal with high-frequency resolution and can accurately estimate the frequency of each part of stator current. This method can effectively shorten the sampling signal's tempo, the performance of its parameter estimation is also superior.a

1 Introduction

Wind power generation in renewable energy, due to its clean, cheap, widely distributed and other characteristics, has received widespread attention from countries around the world. Doubly-fed induction generator (DFIG) is a relatively widely used and mature technology wind turbine [1]. Doubly-fed generators generally have a harsh operating environment and have a high rate of failures. Its stator winding failure rate is high, accounting for 37% of the electrical faults of doubly-fed wind generators [2]. A minor fault will not pose a threat to the power generation system, but it will not be controlled if it is allowed to develop, serious faults will occur. At the same time, the downtime of the power grid has caused great damage to the stability of the power grid. Finding the cause of the fault as soon as possible and tracking and analysing the development trend of the fault in time has great economic benefits for ensuring the safe operation of the wind power system.

In the literature [3], the ellipticity of the Parker vector trajectory is taken as the new fault feature, which can better realise the fault identification of inter-turn short circuit in stator windings. Wei *et al.* [4] extract the negative sequence component of the current estimation difference caused by the inter-turn short-circuit fault of the stator winding. This feature can accurately identify the inter-turn short-circuit coefficient and locate the fault phase, and is robust to non-ideal operation conditions. In the literature [5], the sequential impedance is applied to the fault detection of a doubly-fed machine, which has higher sensitivity and reliability than the traditional feature. All these methods improve the fast Fourier transform (FFT) spectral analysis of the stator current directly.

In the fault signal processing, when the sampling time is short, using the FFT method will result in a certain error. In engineering practice, load fluctuations, noise disturbances and other factors are unavoidable. Extending the signal acquisition time to increase the frequency resolution will inevitably introduce these factors, thereby reducing the accuracy of FFT results [6]. In order to solve the above problems, parametric spectral estimation methods such as ARMA spectral estimation, Pisarenko harmonic decomposition, MUSIC method, Prony method, and minimum norm are applied to the detection of motor fault frequencies. They usually have a higher frequency resolution. Xu and Zhu [7] introduce the MUSIC algorithm into the rotor fault detection of the motor and searches the frequency of the full-frequency signal of the stator current to achieve a high-frequency resolution. Li and Zhu [8] adopt Prony algorithm that combines with difference algorithm, have higher precision and faster operation speed than a traditional FFT algorithm.

This paper combines SVD with TLS-ESPRIT algorithm and proposes a new method for inter-turn fault detection of doubly-fed machines. This method is based on the fact that SVD can filter out the power frequency components of the stator current signal and background noise. TLS-ESPRIT is based directly on the Hankel data matrix composed of data sequences, which avoids the correlation matrix of the signal and simplifies the calculation. It decomposes the signal space into signal subspaces and noise subspaces. Theoretically, it can accurately identify the frequency, amplitude, and phase parameters of any combination of harmonics and interharmonics in the power system, and has strong noise immunity ability. Using MATLAB to build a simulation model to verify the effectiveness of the proposed method.

2 Characteristic analysis of stator inter-turn short circuit

After a short circuit between the stator and the stator of a DFIG, the current flowing through the short-circuited coil is assumed to be $i_g = \sqrt{2}I\cos(\omega t)$, the space electrical angle of the short-circuiting coil along the circumference of the air gap is $\gamma = p\theta$, and the positive and negative magnetomotive forces of the coil of the short-circuit coil occurs after a short-circuit fault occurs between the stator and the coil. The Fourier series expansion of the magnetomotive force is given by the following equation:

$$f(\theta, t) = \frac{\sqrt{2I}}{\pi p}\sum_{v}\frac{1}{v}k_{yv}\cos(\omega t \pm vp\theta) \tag{1}$$

In the formula: k_{yv}, short-circuit pitch factor; p, number of pole pairs; v, harmonic times; θ, the mechanical angle represented by the stator coordinates; φ, rotor coordinates represent the mechanical angle; among them

$$\theta = \varphi + \frac{(1-s)\omega t}{p}.$$

The magnetomotive force $f(\varphi,t)$ of the superimposed current in the short circuit in the rotor coordinate system can be expressed as follows:

$$f(\varphi, t) = \frac{\sqrt{2I}}{\pi p}\sum_{v}\frac{1}{v}k_{yv}\cos(\omega t \pm (1-s)v\omega t \tag{2}$$

The current induced by the magnetomotive force $f(\varphi,t)$ on the rotor side

$$i_R = \sum_v \sqrt{2} I_{Rv} \cos(\omega t \pm (1-s)v\omega t) \tag{3}$$

When the three-phase winding of the motor rotor is symmetrical, the expression of the magnetomotive force generated by the current i_R in the rotor coordinate system is as shown in the following equation:

$$f_R(\varphi, t) = \sum_v \sum_n F_{v,n} \cos[\omega t \pm (1-s)v\omega t - np\varphi] \tag{4}$$

$F_{v,n}$ represents the magnitude of the magnetomotive force for n times of spatial harmonics, $n = 6k+1, k = 0, \pm 1, \pm 2, \ldots$. After coordinate transformation, the expression of the magnetomotive force in $f_R(\varphi,t)$ the stator coordinate system is as shown in the following formula:

$$f_R(\theta, t) = \sum_v \sum_n F_{v,n} \cos\{[1 + (n \pm v)(1-s)]\omega t - np\theta\} \tag{5}$$

After the above analysis, the frequency of the current component of the fault magnetomotive force induced on the rotor side is $[1 \pm v(1-s)]f_1$, where the frequency with a relatively large amplitude have $(2-s)f_1, (2+s)f_1$. The frequency of the current component induced on the stator side is $[(1-s)(1+(n \pm v))]f_1$, where the magnitude of a relatively large amplitude is $3sf_1$ [8] (f_1 represents the fundamental frequency of the stator current).

3 SVD filtering technology

In 1874, Jordan independently derived the singular value decomposition theory of real square matrices. This method has been widely used in many engineering fields [9]. SVD is an algorithm based on singular value classification. The large singular value corresponds to a signal with a large energy or energy concentration. Accordingly, a small singular value corresponds to a signal with smaller energy or energy dispersion [10]. According to the literature [11], the energy of the fundamental frequency component is much larger than the fault characteristic component and the noise energy. Therefore, the SVD filtering technology can filter out the power frequency component, and at the same time, some noise can be filtered out.

For the sampled signal, by the following formula:

$$\boldsymbol{X} = [x(1), x(2), \ldots, x(k), \ldots, x(N)]^H \tag{6}$$

Construct the Hankel matrix

$$\boldsymbol{L} = \begin{bmatrix} x(1) & x(2) & \cdots & x(q) \\ x(2) & x(3) & \cdots & x(q+1) \\ \vdots & \vdots & & \vdots \\ x(p) & x(p+1) & \cdots & x(N) \end{bmatrix} \tag{7}$$

among them, $p + q - 1 = N, q \geq p$, N is the number of sampling points.

Perform singular value decomposition of $\boldsymbol{L}$, as shown in the following equation:

$$\boldsymbol{L} = U\boldsymbol{\Sigma}V^H = U_1 \sum_1 V_1^H + U_2 \sum_2 V_2^H \tag{8}$$

Among them, U and V are the left singular and right singular arrays of the matrix, $\boldsymbol{\Sigma}$ is the $p \times N$ diagonal matrix, and the diagonal elements are the singular values of the matrix $\boldsymbol{L}$. U_1, Σ_1, V_1 correspond to the first few large singular values, which are the parts that need to be filtered out; the superscript H represents the conjugate transpose.

To filter out the power frequency components and noise, two-stage SVD filtering is required. The first stage filters out the power frequency component, that is, performs singular value decomposition on the original signal, retains the large singular value, and performs harmonic recovery based on these large singular values to obtain a pure power frequency component, and then removes the power frequency component from the original signal. The first-order filtered residual signal is obtained, which contains the fault feature component and noise. The second stage filters out the noise, that is, performs singular value decomposition on the filtered residual signal, retains the large singular value, and performs harmonic recovery based on these large singular values to obtain a pure fault feature component [12].

After singular value decomposition of the matrix $\boldsymbol{L}$, the signal is recovered using the simple method shown in (9). After filtering, the first row and last column of the recovery matrix are taken and the first one is turned over for signal reconstruction. Filtered signal recovery sequence

$$\bar{L} = \begin{bmatrix} \bar{x}(1) & \bar{x}(2) & \cdots & \bar{x}(L) \\ \bar{x}(2) & \bar{x}(3) & \cdots & \bar{x}(L+1) \\ \vdots & \vdots & \vdots & \vdots \\ \bar{x}(M) & \bar{x}(M+1) & \cdots & \bar{x}(N) \end{bmatrix} \tag{9}$$

According to (9), the filtered signal is reconstructed to obtain $X = [\bar{x}(1), \bar{x}(2), \ldots \bar{x}(N)]^T$ as the filtered reconstructed signal.

4 TLS-ESPRIT basic theory

The estimating signal parameter via rotational invariance techniques (ESPRIT) is proposed and developed by Roy *et al.* [13, 14]. It was originally used for spatial signal direction of arrival (DOA) estimation, it has now become a sinusoidal signal. Effective tool for estimating parameters (number and frequency). The stability and precision of the ESPRIT algorithm are poor [15]. Therefore, the overall least-squares ESPRIT algorithm is used in the engineering practice, namely TLS-ESPRIT [16]; this paper uses the TLS-ESPRIT algorithm.

The sampled signal $x(n)$ can be represented as a combination of a series of cosine harmonic components, as shown in the following formula:

$$x(n) = \sum_{i=1}^{p} A_i \cos(2\pi f_i n T_s + \phi_i) \quad n = 1, 2, \ldots, N \tag{10}$$

In the formula, T_s represents the sampling period, N is the number of sampling points, p is the number of harmonics; A_i, f_i,Φ_i represent the amplitude, frequency, and initial phase angle of the harmonic.

Define $y(n) = x(n+1)$, and let the following $m \times N$-order matrix (guarantee $m \geq p$):

$$X(n) = (x(n)x(n+1)\cdots x(n+m-1))^T \tag{11}$$

$$Y(n) = (y(n)y(n+1)\cdots y(n+m-1))^T \tag{12}$$

The autocorrelation matrix of $X(n)$ is the following equation:

$$\boldsymbol{R}_{XX} = E[X(n)X^H(n)] \tag{13}$$

The cross-correlation matrix of $X(n)$ and $Y(n)$ is the following equation:

$$\boldsymbol{R}_{XY} = E[X(n)Y^H(n)] \tag{14}$$

where E represents the mathematical expectation and H represents the conjugate transpose. Perform eigenvalue decomposition on $\boldsymbol{R}_{XX}$, determine its minimum eigenvalue σ^2, and calculate $R_1 = \boldsymbol{R}_{XX}$

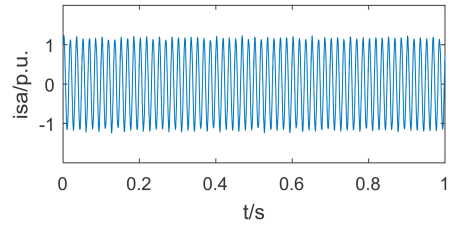

Fig. 1 *Stator a-phase fault current waveform*

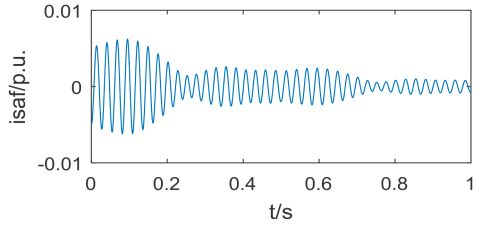

Fig. 2 *Rotor a-phase fault current waveform*

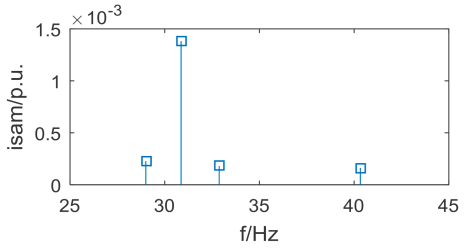

Fig. 3 *Stator fault signal after SVD filtering*

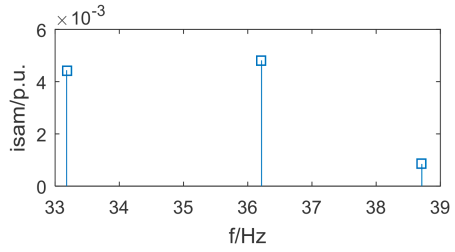

Fig. 4 *Stator a-phase normal current spectrum (TLS-ESPRIT)*

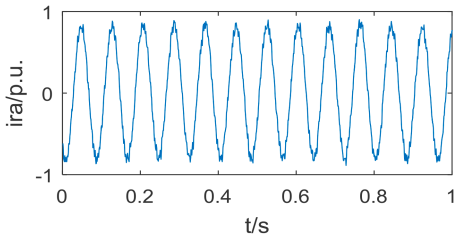

Fig. 5 *Stator a-phase current spectrum (TLS-ESPRIT)*

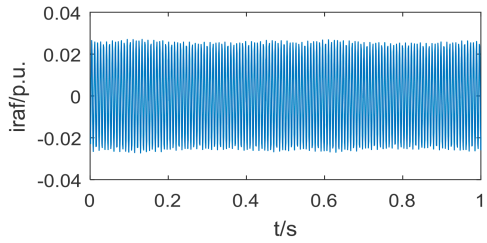

Fig. 6 *Rotor fault signal after SVD filtering*

$-\sigma^2\boldsymbol{I}$, ($\boldsymbol{I}$ denotes an m-order matrix); Singular value decomposition $R_1 = U\,\boldsymbol{\Sigma}\,V^H$ for R_1, where

$$U = (U_1 U_2), \boldsymbol{\Sigma} = \begin{bmatrix} \boldsymbol{\Sigma}_1 & 0 \\ 0 & \boldsymbol{\Sigma}_2 \end{bmatrix}$$

(Σ_1 consists of p main singular values)

$$V^H = \begin{bmatrix} V_1^H \\ V_2^H \end{bmatrix}.$$

Calculate $R_2 = R_{XY} - \sigma^2 Z$, $\boldsymbol{Z}$ denotes an m-order matrix

$$\boldsymbol{Z} = \begin{bmatrix} 0 & 0 \\ I_{m-1} & 0 \end{bmatrix}$$

(here I_{m-1} represents the $m-1$ order unit array). Calculate the matrix $\boldsymbol{U}_1^H \boldsymbol{R}_2 \boldsymbol{V}_1$ and perform generalised eigenvalue decomposition on $\{\sum_1 \boldsymbol{U}_1^H \boldsymbol{R}_2 \boldsymbol{V}_1\}$ to determine p generalised eigenvalues $\lambda_i (i = 1, 2, \ldots, p)$ (the remaining m–p generalised eigenvalues are always equal to 0). According to the generalised eigenvalues, the frequency $f_i = (1/2\pi)\arctan(\mathrm{Im}(\lambda_i)/\mathrm{Re}(\lambda_i))$ of each component of the sampled signal is determined, and $\mathrm{Im}(\lambda_i)$ and $\mathrm{Re}(\lambda_i)$ represent the imaginary and real parts of the eigenvalues, respectively.

Define the matrix $\boldsymbol{\lambda}$:

$$\boldsymbol{\lambda} = \begin{bmatrix} 1 & 1 & \cdots & 1 \\ \lambda_1 & \lambda_2 & \cdots & \lambda_p \\ \vdots & \vdots & & \vdots \\ \lambda_1^{N-1} & \lambda_2^{N-1} & \cdots & \lambda_p^{N-1} \end{bmatrix} \tag{15}$$

Calculate the matrix $\boldsymbol{c} = (\lambda^H \boldsymbol{\lambda})^{-1} \lambda^H X$, where $\boldsymbol{c}$ is a list of vectors $\boldsymbol{c} = (c_1\ c_2 \cdots c_p)^T$ and $\boldsymbol{X}$ is the column vector $(x(1)\ x(2) \cdots x(N))^T$. The amplitude and initial phase angle of each component of the sampled signal are determined to be: $A_i = 2|c_i|$, $\phi_i = \arctan(\mathrm{Im}(\lambda_i)/\mathrm{Re}(\lambda_i)), i = 1, 2, \ldots, p$

5 Simulation verification

The basic parameters of the DFIG simulated in this paper are as follows: rated voltage is 575 V, rated frequency is 60 Hz, pole pair number is 3, and the stator phase resistance is 0.023 p.u., the rotor resistance per phase is 0.016 p.u., the stator leaks per phase is 0.18 p.u., the rotor leakage inductance is 0.16 p.u., the mutual inductance between stator and rotor is 2.9 p.u., and the short circuit resistance between turns is 0.01 Ω. Wang [17] has detailed the DFIG model under normal and stator inter-turn faults, which will not be described in detail here. In the simulation, a coil in the stator a phase has a short circuit in the inter-turn, and a fault occurs in 2 s. The wind speed is set to 13.2 m/s and the slip rate is −0.2.

Set the ratio of the short-circuit turns of the stator winding inter-turn turn-to-turn short-circuit turns (the ratio of the short-circuit turns to the total turns of the coil) is 0.15. Under normal conditions, the stator winding current is symmetric, and the frequency of the stator current fundamental wave is f = 60 Hz when the slip ratio. When −0.2, the frequency of the rotor-side current fundamental wave is f = −12 Hz. When the stator winding has a turn-to-turn fault and reaches a steady state, the stator-rotor current waveform is shown in Figs. 1 and 2. Taking the number of sampling points N = 1000, sampling time t = 1 s, sampling frequency f_s = 1000 Hz, performing SVD filtering on current signals and analysing with ESPRIT algorithm. The results are shown in Figs. 3–8.

Fig. 1 shows the stator current a-phase current waveform in case of a fault, Fig. 3 shows the fault current signal after a phase current filtering by SVD, and Fig. 4 shows a normal stator a phase current estimated by TLS-ESPRIT algorithm after SVD filtering. Fig. 5 shows the fault current filtered by SVD using TLS-ESPRIT algorithm. Detecting the frequency of the fault eigenfrequency on the stator side (36 Hz), we can see from Table 1 that the parameter estimation performance of SVD filter-TLS-ESPRIT and FFT (10 s) is consistent, because the SVD filter-TLS-ESPRIT method makes the fault component complex (see Table 2). The background noise is extracted to improve the detection accuracy and accuracy. The

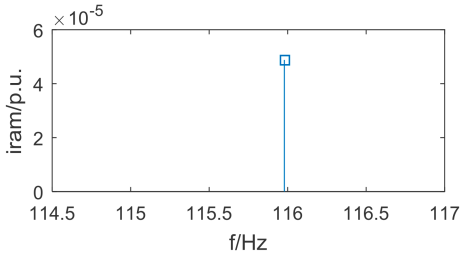

Fig. 7 *Rotor a-phase normal current spectrum (TLS-ESPRIT)*

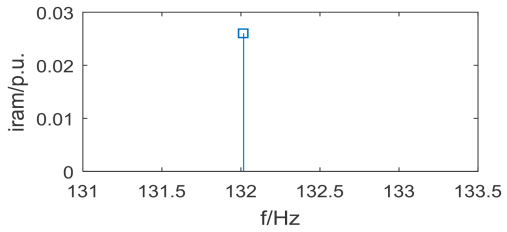

Fig. 8 *Rotor a-phase current spectrum (TLS-ESPRIT)*

Table 1 Stator side a-phase current simulation results

Variable	SVD-TLS-ESPRIT (1 s)	FFT (10 s)	ESPRIT (1.1 s)
$3sf_1$, Hz	36.20	36.01	35.89
$3sf_1$ component amplitude, p.u.	0.0048	0.0046	0.0040

Table 2 Rotor side a-phase current simulation results

Variable	SVD-TLS-ESPRIT (1 s)	FFT (10 s)	ESPRIT (1.1 s)
$(2-s)f_1$, Hz	132.02	132	132.015
$(2-s)f_1$ component amplitude, p.u.	0.026	0.026	0.021

accuracy of ESPRIT's analysis of fault components is obviously insufficient.

Fig. 2 shows the rotor current a-phase current waveform in case of fault, Fig. 6 shows the fault current signal after the a-phase current is filtered by SVD, and Fig. 7 shows a normal rotor a-phase current estimated by TLS-ESPRIT algorithm after SVD filtering. Fig. 8 shows the fault current filtered by SVD using TLS-ESPRIT algorithm. From Fig. 8, it is known that the rotor current fault amplitude of DFIG stator winding fault is larger, and its main fault characteristic frequency is $(2-s)f_1$ (132 Hz in this paper), its ESPRIT algorithm analysis results are consistent with the stator side analysis.

The analysis shows that it is feasible to apply the combination of SVD filtering and TLS-ESPRIT algorithm to the stator inter-turn fault detection of doubly fed induction generator, and because only a short time data (1 s) can be used to guarantee the performance of the stator inter-turn short-circuit fault detection, so the performance of fault detection is inferred to be applicable to adverse conditions such as load fluctuations and noise interference.

6 In conclusion

In this paper, SVD filtering and TLS-ESPRIT algorithm are applied to the fault detection of the stator inter-turn short circuit of the DFIG. Using SVD filtering technology to preprocess the data, a very pure fault characteristic component can be obtained, then the filtered signal is analysed by TLS-ESPRIT algorithm, and the ideal estimation result can be obtained, and only need a short-time sampling data to effectively detect the fault feature frequency. Due to its simple algorithm and short runtime, it is more suitable for online detection.

7 References

[1] Wang, H., Zhang, W., Hu, J., *et al.*: 'A control strategy for doubly-fed induction generator wind turbines under asymmetrical grid voltage conditions caused by faults', *Electr. Power Autom. Equip.*, 2010, **34**, (4), pp. 97–102

[2] Wang, Z., Xu, Y., Liu, S., *et al.*: '*Large wind turbine condition monitoring and intelligent fault diagnosis*', vol. 58 (Shanghai Jiao Tong University Press, Shanghai, 2013)

[3] Wei S. Li, Z., *et al.*: 'Inter-turn faults diagnosis on stator windings of offshore wind DFIGs considering current estimated difference', *Proc. CSEE*, 2018, pp. 1–9

[4] Wei, S., Zhang, L., Fu, Y., *et al.*: 'Early fault detection based on the quasi-sequence impedance for inter-turn faults in stator windings of offshore wind DFIG', *Proc. CSEE*, 2017, **37**, (1), pp. 273–282, https://doi.org/10.13334/j.0258-8013.pcsee.170988, accessed June 2019

[5] Ma, H., Zhang, Z., Shi, W., *et al.*: 'Doubly-fed induction generator stator fault diagnosis based on rotor instantaneous power spectrum', *Autom. Electr. Power Syst.*, 2014, **38**, (14), pp. 30–35

[6] Xu, B., Sun, L.: 'Concurrent discrimination of rotor fault and load oscillation in induction motors', *Proc. CSEE*, 2016, **36**, (23), pp. 6518–6527o+6619

[7] Xu, B., Zhu, M.: 'A new detection method for broken rotor bar fault in squirrel cage induction motors based on SFOC-MUSIC and hybrid genetic algorithm', *Electric Mach. Control Appl.*, 2016, **43**, (7), pp. 73–80o+85

[8] Li, J.Q., Zhu, J.: 'Characteristic analysis of stator inter-turn short circuit fault in doubly-fed induction generator based on prony', *Electric Mach. Control Appl.*, 2016, **43**, (7), pp. 86–91

[9] Zhang, X.: '*Matrix analysis and application*' (Tsinghua University Press, Beijing, 2004)

[10] Zhao, X., Ye, B, Chen, T.: 'Extraction method of faint fault feature based on wavelet-SVD difference spectrum', *J. Mech. Eng.*, 2012, **48**, (7), pp. 37–48

[11] Deleroi, W.: 'Broken bar in squirrel cage rotor of an induction motor, part 1: description by supermposed fault currents', *Archivfur Elektrotechnik*, 1984, **67**, pp. 91–99

[12] Bai, X.: '*The ESPRIT-based detection method for broken rotor bar fault in induction motors*' (North China Electric Power University, Baoding, China, 2014)

[13] Roy, R., Paulraj, A., Kailath, T.: 'ESPRIT-a subspace rotation approach to estimation of parameters of cissoids in noise', *IEEE Trans. Acoust. Speech Signal Process.*, 1986, **34**, (5), pp. 1340–1342

[14] Roy, R., Kailath, T.: 'Prefiltering-based ESPRIT for estimating sinusoidal in non-Gaussian ARMA noise', *IEEE Trans. Signal Process.*, 1995, **43**, (1), pp. 349–353

[15] Roy, R., Kailath, T.: 'ESPRIT-estimation of signal parameters via rotational invariance techniques', *IEEE Trans. Acoust. Speech Signal Process.*, 1989, **37**, (7), pp. 984–995

[16] Zhang, J., Xu, Z., Niu, L.: 'Application of TLS-ESPRIT in high resolution spectrum estimation of power system signal', *Electr. Power Autom. Equip.*, 2009, **29**, (5), pp. 48–51

[17] Wang, J.: '*Analysis of the characteristics of the fault in doubly-fed induction generators and detection scheme research*' (North China Electric Power University, Baoding, China, 2015)